Supplementary Information

Wilver A. Muriel,[†] Trinidad Novoa,[‡] Carlos Cárdenas,[†] and Julia Contreras-García[*,‡]

†*Departamento de Física, Facultad de Ciencias, Universidad de Chile, Chile.*

‡*Laboratoire de Chimie Théorique, Sorbonne Université & CNRS, 4 Pl. Jussieu, 75005, Paris, France*

¶*Centro para el Desarrollo de la Nanociencia y la Nanotecnología (CEDENNA), RM 9170124, Santiago, Chile*

E-mail: contrera@lct.jussieu.fr

SC-DFT

The extensive application of Density Functional Theory (DFT) in electronic structure calculations, owing to its effective balance between precision and computational efficiency, has prompted its expansion to diverse systems. Superconductors present a distinctive case as they cannot be addressed perturbatively due to the broken phase symmetry, which means the conservation of particle numbers is not guaranteed. Additionally, superconductors exhibit significant electron-phonon coupling, necessitating the consideration of ionic displacements around equilibrium positions in the Hamiltonian. Thus, in Superconducting Density Functional Theory (SC-DFT), the nuclear dynamics must be incorporated, as detailed in references[1–4].

In brief, the purely ionic segment of the Hamiltonian is expressed using ionic field operators,

$\Phi(\boldsymbol{R})$, encompassing kinetic and interaction terms:

$$\hat{H}_i = - \int \Phi^\dagger(\boldsymbol{R}) \frac{\nabla^2}{2M} \Phi(\boldsymbol{R}) d\boldsymbol{R} \tag{1}$$

$$+ \frac{1}{2} \int \Phi^\dagger(\boldsymbol{R}) \Phi^\dagger(\boldsymbol{R}') \frac{Z}{|\boldsymbol{R} - \boldsymbol{R}'|} \Phi(\boldsymbol{R}') \Phi(\boldsymbol{R})\, d\boldsymbol{R}\, d\boldsymbol{R}' \,. \tag{2}$$

Meanwhile, the electron-ion interaction is described by:

$$\hat{H}_{ie} = -\frac{1}{2} \sum_\sigma \int \psi^\dagger_\sigma(\boldsymbol{r}) \Phi^\dagger(\boldsymbol{R}) \frac{Z}{|\boldsymbol{R} - \boldsymbol{r}|} \Phi(\boldsymbol{R}) \psi_\sigma(\boldsymbol{r})\, d\boldsymbol{R}\, d\boldsymbol{r} \,. \tag{3}$$

The electronic part of the Hamiltonian takes the form:

$$\hat{H}_e = \sum_\sigma \int \psi^\dagger_\sigma(\boldsymbol{r}) \left[-\frac{\nabla^2}{2} - \mu \right] \psi_\sigma(\boldsymbol{r})\, d\boldsymbol{r} \tag{4}$$

$$+ \frac{1}{2} \sum_{\sigma\sigma'} \int \psi^\dagger_\sigma(\boldsymbol{r}) \psi^\dagger_{\sigma'}(\boldsymbol{r}') \frac{1}{|\boldsymbol{r} - \boldsymbol{r}'|} \psi_\sigma(\boldsymbol{r}) \psi_{\sigma'}(\boldsymbol{r}')\, d\boldsymbol{r}\, d\boldsymbol{r}' \,. \tag{5}$$

Additionally, three external potentials are considered: one coupling to electrons, one to ions, and an anomalous potential, $\Delta_{ext}(\boldsymbol{r}, \boldsymbol{r}')$, responsible for symmetry breaking, allowing Cooper pairs' tunneling. If $\Delta_{ext}(\boldsymbol{r}, \boldsymbol{r}')$ tends towards zero, the Hamiltonian converges to a non-superconducting state. Thus, SC-DFT enables the control of superconductivity and facilitates the comparison of system properties in normal and superconducting states. Similar to conventional DFTs, a Hohenberg-Kohn theorem establishes a one-to-one correspondence between the external potentials and corresponding densities. The inclusion of the anomalous potential necessitates working within the grand-canonical ensemble.

Another Hohenberg-Kohn-like theorem demonstrates that the grand-canonical potential follows a variational principle concerning the densities. This potential incorporates kinetic and entropy terms, along with system-independent functionals, resembling universal DFT functionals. The explicit form of this functional remains unknown, necessitating the introduction of a reference (Kohn-Sham) system. The resulting equations lead to expressions for ions and electronic Hamiltonians.

In the superconducting state, the electron density is expressed as a summation over occupied states, considering their respective occupation numbers. The difference in electron densities between normal and superconducting states is expressed as a variation in occupation numbers. It can then be shown[5] that the electron density in the superconducting state becomes:

$$\rho^{SC}(\boldsymbol{r}) = \sum_{n\boldsymbol{k}} n_{n\boldsymbol{k}}^{SC} |\varphi_{n\boldsymbol{k}}(\boldsymbol{r})|^2 \,, \tag{6}$$

where

$$n_{n\boldsymbol{k}}^{SC} = 1 - \frac{\xi_{n\boldsymbol{k}}}{|E_{n\boldsymbol{k}}|} \tanh\left(\frac{\beta\,|E_{n\boldsymbol{k}}|}{2}\right). \tag{7}$$

Notice that in the normal state limit, $\Delta_s(n\boldsymbol{k}) \to 0$, we recover the normal state density, so that we can express the difference in the electron densities when going from the normal to the superconductor state as a difference in the occupation numbers, $\Delta n = n_{n\boldsymbol{k}}^{SC} - n_{n\boldsymbol{k}}^{SC}$:

$$\rho^{SC}(\boldsymbol{r}) - \rho^{NS}(\boldsymbol{r}) = \sum_{n\boldsymbol{k}} (n_{n\boldsymbol{k}}^{SC} - n_{n\boldsymbol{k}}^{SC}) |\varphi_{n\boldsymbol{k}}(\boldsymbol{r})|^2 \,. \tag{8}$$

Δn is illustrated in Figure 1 for Δ=10 meV and β=0.3 meV^{-1}. It can be seen that the difference is very small.

Figures

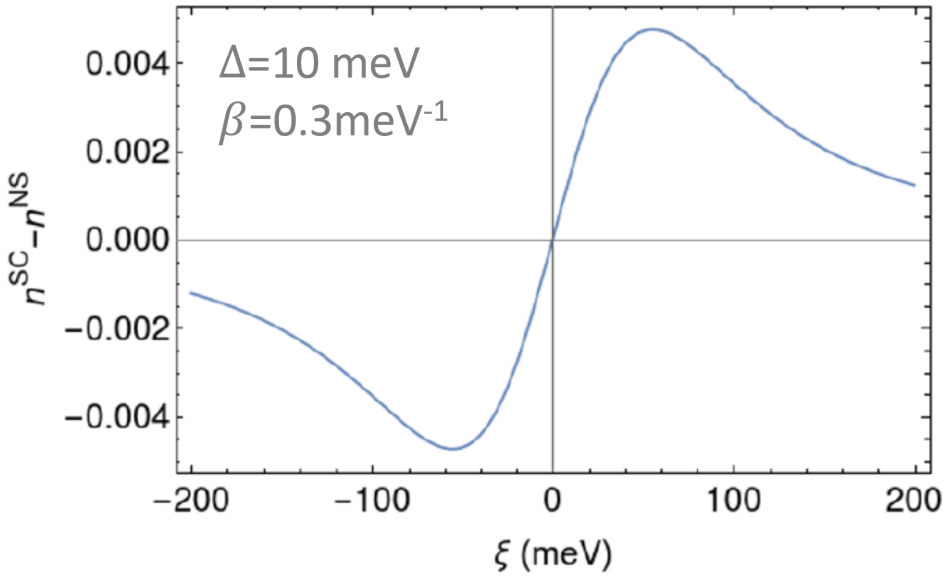

Figure 1: Difference between the occupation numbers of the superconducting and normal states with respect to the normal state energies, ξ, for a given gap of $\Delta = 10$ meV (at T=0 K), and $\beta = 0.3$ meV^{-1}.

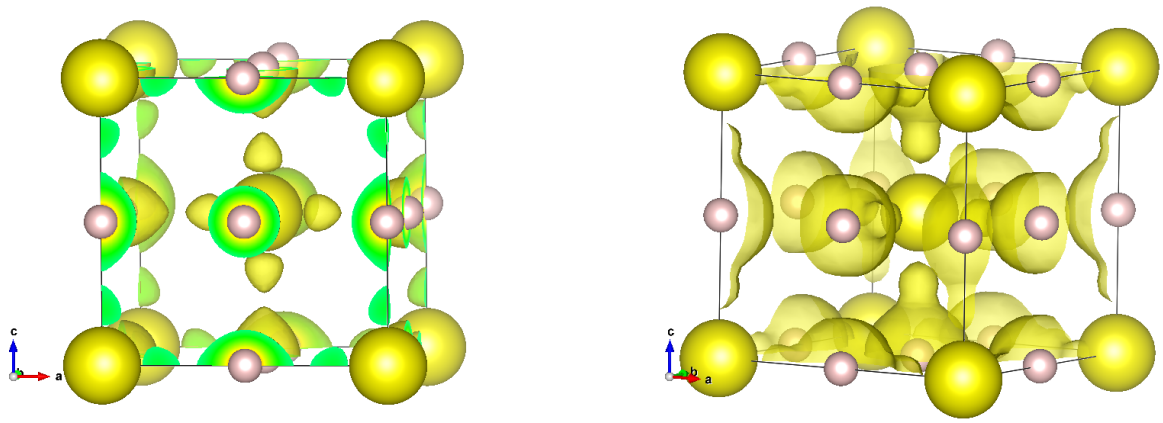

Figure 2: H_3S isosurfaces at T=200K. Left: ρ=0.002 a.u. Right: ELF=0.005.

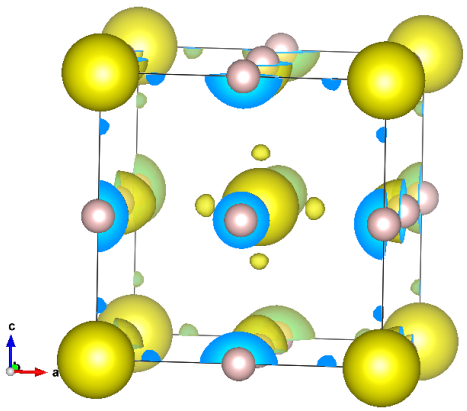

Figure 3: H_3S 0.0008 density difference isosurface (10-200K).

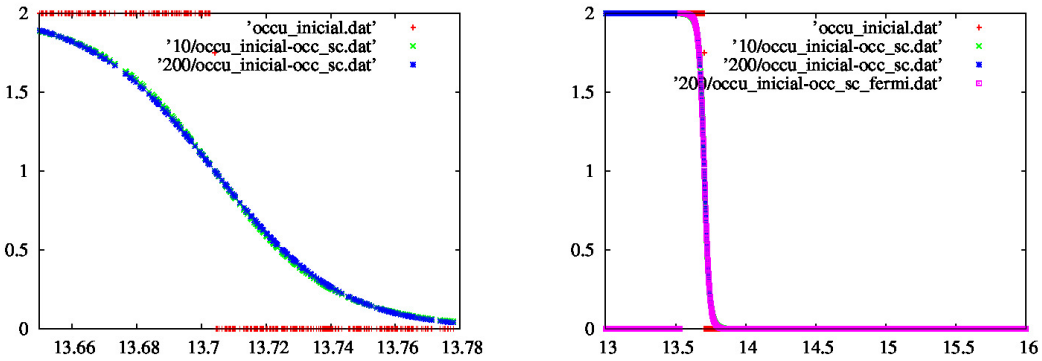

Figure 4: Occupations at T=10K and T=200K in the superconducting state. The normal state has also been added as a reference. The calculation around the Fermi level is shown in the right pannel.

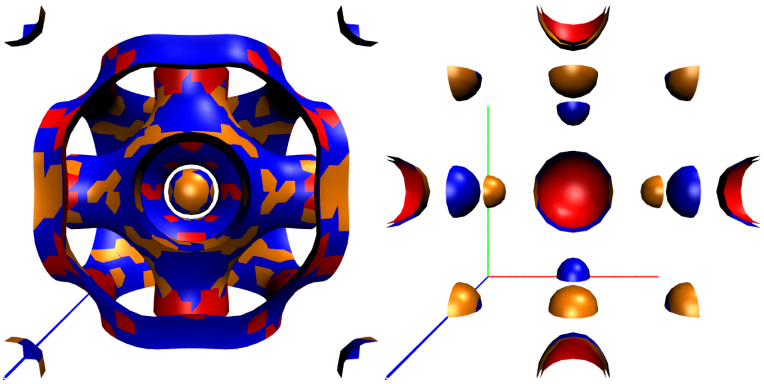

Figure 5: H_3S isosurfaces at 10K (blue), 100K (orange) and 200K (red). Left: ELF=0.5; . Right: ELF_{FL}=0.1

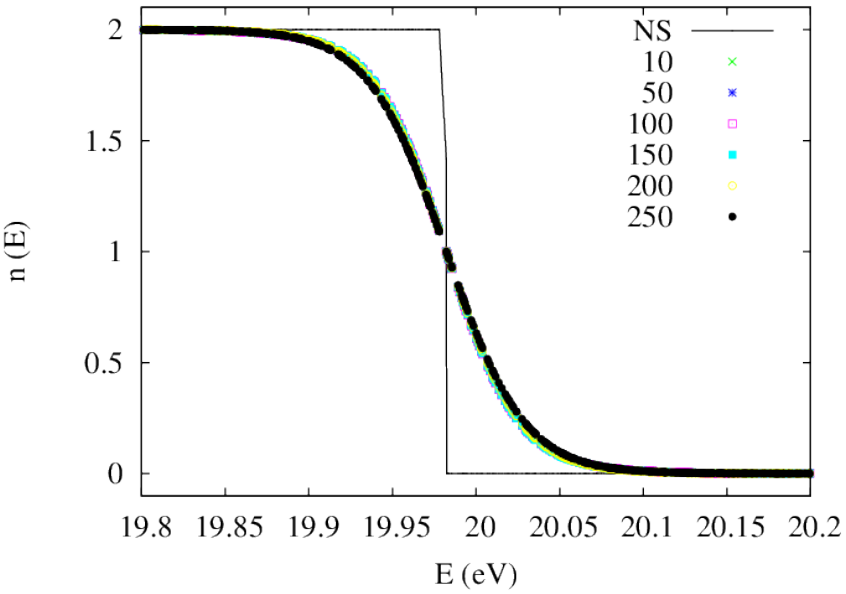

Figure 6: Occupations LaH_{10}

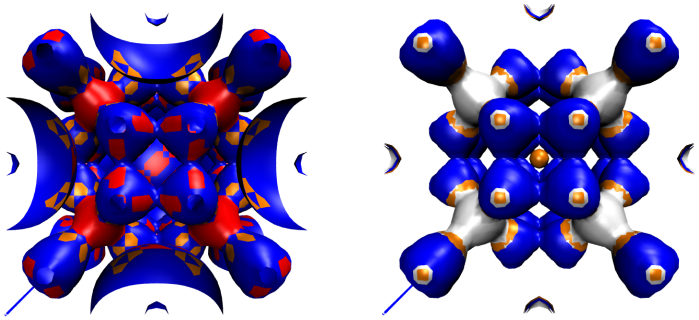

Figure 7: LaH_{10} isosurfaces at 10K (blue), 100K (orange) and 250K (red). Left: ELF=0.5 a.u; . Right: ELF_{FL}=0.001 a.u.

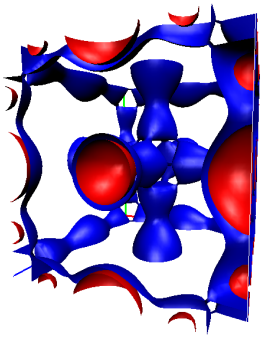

Figure 8: ρ_{FL}=0.0022 a.u. at different temperatures in H_3S: 10K in blue and 200K in red.

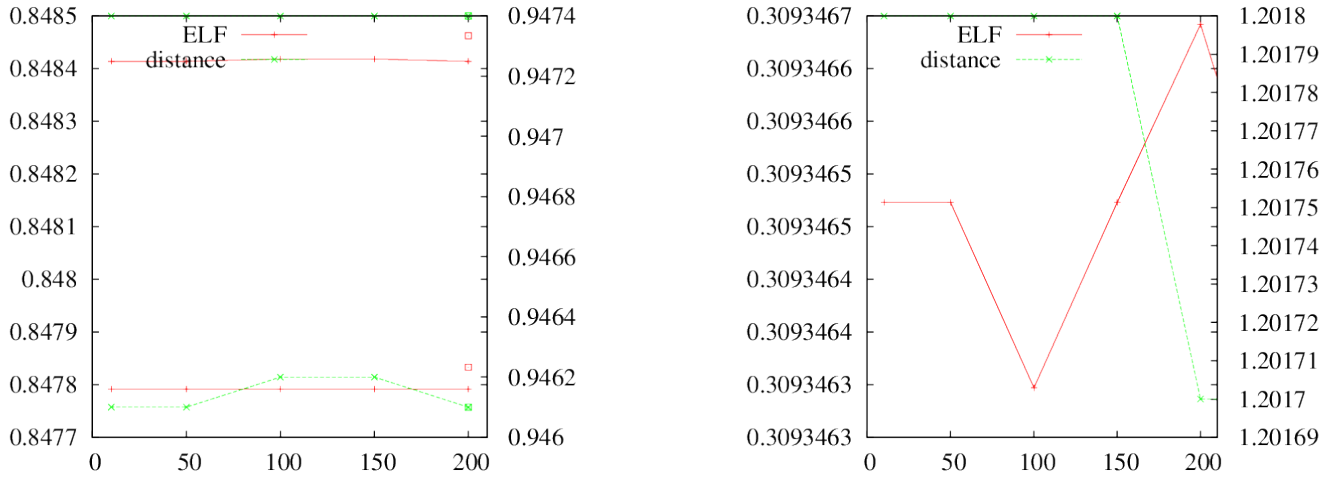

Figure 9: ELF values (red line, left axis) and distances to nearest atom in a.u. (green line, right axis) of the hydrogen saddle points.

References

(1) Oliveira, L. N.; Gross, E. K. U.; Kohn, W. Density-Functional Theory for Superconductors. *Phys. Rev. Lett.* **1988**, *60*, 2430–2433.

(2) Oliveira, L. N.; Gross, E. K. U.; Kohn, W. Density-Functional Theory for Superconductors. *Phys. Rev. Lett.* **1988**, *60*, 2430–2433.

(3) Sanna, A. In *Introduction to Superconducting Density Functional Theory*; Pavarini, E., Koch, E., Scalettar, R., Martin, R., Eds.; The Physics of Correlated Insulators, Metals, and Superconductors; Forschungszentrum Jülich, 2017; Vol. 7.

(4) Sanna, A.; Pellegrini, C.; Gross, E. K. U. Combining Eliashberg Theory with Density Functional Theory for the Accurate Prediction of Superconducting Transition Temperatures and Gap Functions. *Phys. Rev. Lett.* **2020**, *125*, 057001.

(5) Novoa, T.; di Mauro, M.; Errea, I.; Braïda, B.; Contreras-García, J. Molecularity: a fast and efficient criterion for probing superconductivity. *submitted*